

# Fermi surface and spectral functions of a hole-doped spin-fermion model for cuprates

Mohammad Moraghebi,<sup>1</sup> Charles Buhler,<sup>1</sup> Seiji Yunoki,<sup>2</sup> and Adriana Moreo<sup>1</sup>

<sup>1</sup>*Department of Physics, National High Magnetic Field Lab and MARTECH, Florida State University, Tallahassee, Florida 32306*

<sup>2</sup>*Materials Science Center, University of Groningen, Nijenborgh 4, 9747 AG Groningen, The Netherlands*

(Received 16 November 2000; published 10 May 2001)

Using numerical techniques we study the spectral function  $A(k, \omega)$  of a spin-fermion model for cuprates in the regime where magnetic and charge domains (stripes) are developed upon hole doping. From  $A(k, \omega)$  we study the electronic dynamics and determine the Fermi surface (FS), which is compared with angular-resolved photoemission results for  $\text{La}_{2-x}\text{Sr}_x\text{CuO}_2$ . A pseudogap is observed in the density of states at the chemical potential for all finite dopings. The striped ground state appears to be metallic in this model since there is finite spectral weight at the chemical potential, but the electronic hopping seems to be stronger perpendicular to the stripes rather than along them. The band structure is not rigid, contrary to the behavior found in mean-field studies, and changes with doping. Both midgap (stripe-induced) and valence-band states determine the FS. For vertical (horizontal) stripes, a clear FS appears close to  $(\pi, 0)$  [ $(0, \pi)$ ], while no FS is observed close to  $(0, \pi)$  [ $(\pi, 0)$ ]. Along the diagonal direction the spectral function shows a clear quasiparticle peak close to  $(0, 0)$ , but its weight is reduced as the chemical potential is approached. A weak FS develops along this direction as the system is doped.

DOI: 10.1103/PhysRevB.63.214513

PACS number(s): 74.20.Mn, 74.72.-h, 71.10.Fd

## I. INTRODUCTION

Neutron-scattering studies have shown that many high-temperature superconducting materials exhibit magnetic incommensurability (IC) upon hole doping.<sup>1</sup> In some compounds it is believed that this spin IC is due to the formation of charge stripes.<sup>2</sup> Indirect evidence of static stripe formation has been observed in Nd-doped  $\text{La}_{2-x}\text{Sr}_x\text{CuO}_2$  (LSCO).<sup>2</sup> On the other hand, in LSCO, angular-resolved photoemission experiments (ARPES) (Ref. 3) as well as neutron scattering<sup>4</sup> show features consistent with the existence of dynamical stripes. In neutron scattering the evidence is in the broadening of the peak in the supposedly inhomogeneous stripe regime, while in ARPES a one-dimensional-like band dispersion and a straight Fermi surface (FS) around  $(\pi, 0)$  and  $(0, \pi)$  are observed.

The goal of this paper is to gain theoretical understanding on the effect of stripes in the spectral function and FS of a system of electrons and spins, since these are properties that can be measured in ARPES experiments. In previous attempts to study these properties, mean-field and exact diagonalization (ED) techniques have been applied to the Hubbard and  $t$ - $J$  models.<sup>5-7</sup> The problem with these models is that it has not been shown that their actual ground state has striped characteristics. In mean-field approaches<sup>5</sup> not all possible states have been considered, and with ED, additional attractive terms have to be added to the Hamiltonian to stabilize the striped phase.<sup>6</sup> Thus, here we consider a spin-fermion model that can be unbiasedly studied with accurate Monte Carlo (MC) techniques without “sign problems” and, upon hole doping, has a striped ground state, as shown in previous investigations.<sup>8,9</sup> This model has been used successfully to qualitatively describe magnetic and charge properties of the cuprates, showing that spin IC and charge stripe formation are related.<sup>8,9</sup>

The main result of the present effort is that midgap states associated with the stripes and valence-band states related to

the background both contribute to determine the FS. The band structure is not rigid, as found in mean-field calculations.<sup>5</sup> A pseudogap at the chemical potential clearly develops as the system is doped. The doped holes are not only introduced into the stripes but also into the background, and the striped state appears to be metallic, although the electronic hopping is stronger along the direction perpendicular to the stripes.

The paper is organized as follows: the spin-fermion model is presented in Sec. II, a schematic picture is shown in Sec. III, and Sec. IV is devoted to the results. The pseudogap is discussed in Sec. V, and the conclusions are presented in Sec. VI.

## II. THE MODEL

The spin-fermion model is constructed as an interacting system of electrons and spins, crudely mimicking phenomenologically the coexistence of charge and spin degrees of freedom in the cuprates.<sup>10-12</sup> Its Hamiltonian is given by

$$H = -t \sum_{\langle \mathbf{i} \mathbf{j} \rangle \alpha} (c_{i\alpha}^\dagger c_{j\alpha} + \text{H.c.}) + J \sum_{\mathbf{i}} \mathbf{S}_{\mathbf{i}} \cdot \mathbf{S}_{\mathbf{i}} + J' \sum_{\langle \mathbf{i} \mathbf{j} \rangle} \mathbf{S}_{\mathbf{i}} \cdot \mathbf{S}_{\mathbf{j}}, \quad (1)$$

where  $c_{i\alpha}^\dagger$  creates an electron at site  $\mathbf{i} = (i_x, i_y)$  with spin projection  $\alpha$ ,  $\mathbf{S}_{\mathbf{i}} = \sum_{\alpha\beta} c_{i\alpha}^\dagger \boldsymbol{\sigma}_{\alpha\beta} c_{i\beta}$  is the spin of the mobile electron, the Pauli matrices are denoted by  $\boldsymbol{\sigma}$ ,  $\mathbf{S}_{\mathbf{i}}$  is the localized spin at site  $\mathbf{i}$ ,  $\langle \mathbf{i} \mathbf{j} \rangle$  denotes nearest-neighbor (NN) lattice sites,  $t$  is the NN-hopping amplitude for the electrons,  $J > 0$  is an antiferromagnetic (AF) coupling between the spins of the mobile and localized degrees of freedom at the same site, and  $J' > 0$  is a direct AF coupling between the localized spins in nearest-neighbor sites. The density  $\langle n \rangle = 1 - x$  of itinerant electrons is controlled by a chemical potential  $\mu$ . Hereafter  $t = 1$  will be used as the unit of energy. From previous phenomenological analysis the coupling  $J$  is expected

to be larger than  $t$ , while the Heisenberg coupling  $J'$  is expected to be smaller.<sup>11,12,8</sup> The value of  $J$  will be here fixed to 2 and the coupling  $J' = 0.05$ , as in Ref. 8. To simplify the numerical calculations, avoiding the sign problem, the localized spins are assumed to be classical (with  $|\mathbf{S}_i| = 1$ ). This approximation was discussed in detail in Ref. 8 and it is not expected to alter qualitatively the behavior of the striped ground state. The model will be studied using a standard MC method, details of which can be found in Ref. 13. Periodic boundary conditions are used.

The spectral function  $A(k, \omega)$  is defined as

$$A(k, \omega) = -\frac{1}{\pi} \text{Im} G(k, \omega), \quad (2)$$

where  $G(k, \omega)$  is the one-particle retarded Green's function for the electrons,  $k$  is the momentum, and  $\omega$  denotes the energy. Since we are performing a MC calculation on the classical spins only, because the fermions do not interact among themselves directly but only through the classical spins, the time-dependent Green's function can be straightforwardly calculated in real time. The spectral functions obtained with this procedure only contain small controlled statistical errors. This should be contrasted against other calculations that use the maximum entropy technique, which is typically an uncontrolled procedure. The density of states (DOS)  $N(\omega)$  is obtained by adding the spectral functions for all different momenta in the first Brillouin zone (FBZ).

### III. SCHEMATIC PICTURE

ARPES results in  $\text{La}_{1.28}\text{Nd}_{0.6}\text{Sr}_{0.12}\text{CuO}_4$  show a FS that appears to be formed by the superposition of two one-dimensional (1D) FS's believed to be caused by metallic stripes in an insulating background.<sup>14</sup> Similar features are observed in underdoped LSCO<sup>3</sup> and in  $\text{Bi}_2\text{Sr}_2\text{CaCu}_2\text{O}_{8+y}$  ( $\text{Bi}2212$ ).<sup>15</sup> The naive band structure that would provide such a FS is shown in Fig. 1(a), along the main directions in the FBZ, for the case of quarter-filled (metallic) equally spaced vertical stripes with a period  $a=4$  on an AF (insulating) background. The overall density is  $\langle n \rangle = 0.875$ , which corresponds to a hole density  $x = 0.125$ . A valence and conduction band, separated by the AF gap, are associated with the insulating background. The dashed line indicates "shadow bands."<sup>16</sup> In the middle of the gap there is a band that corresponds to the 1D stripes. Notice that the midgap band is not symmetric under  $\pi/2$  rotations. At  $(\pi, 0)$  [ $(0, \pi)$ ] the midgap band is closer to the valence (conduction) band. The midgap-band energy is given by  $E_m(k_x, k_y) = -t' \cos k_y$ , while the energy of the valence and conduction bands is given by  $E_k^\pm = \pm \sqrt{\epsilon_k^2 + \Delta^2}$ , where  $\epsilon_k = -2t(\cos k_x + \cos k_y)$ , and  $2\Delta$  is the AF gap. In Fig. 1(a) we have used  $t' = 0.5$ ,  $t = 1$ , and  $\Delta = 1$  for simplicity. The metallic band is crossed by the Fermi energy ( $E_F$ ) defining the FS shown in Fig. 1(b). Notice that the midgap band is flat, i.e., it does not disperse, along  $(0, \pi) - (\pi, \pi)$  and  $(0, 0) - (\pi, 0)$  indicating that the holes are static in the horizontal direction (they only can move vertically along the stripe). The corresponding schematic density of states is shown in Fig. 1(c).

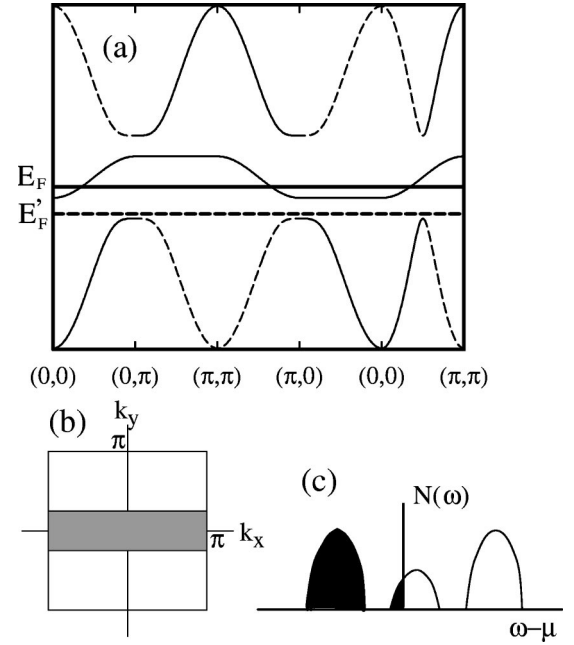


FIG. 1. (a) Schematic band structure along the path  $(0,0) - (0,\pi) - (\pi,\pi) - (\pi,0) - (0,0) - (\pi,\pi)$  in the FBZ for an AF system with metallic quarter-filled vertical stripes with  $\langle n \rangle = 0.875$ .  $E_F$  indicates the position of the Fermi energy and shadow bands are indicated by a dashed line.  $E'_F$  indicates the position of the Fermi energy in the case of empty ( $\langle n \rangle = 0$ ) stripes. (b) Fermi surface corresponding to the band structure shown in (a). (c) The corresponding density of states of (a).

This naive picture also shows that if the hole density of the stripes were 1 rather than 0.5 the system would be insulating since, as shown in Fig. 1(a), the Fermi energy, indicated by  $E'_F$ , would be inside a gap and all the stripe states would be empty. When typical mean-field calculations allowing for the possibility of vertical stripes are performed on the Hubbard model, the stable solution is qualitatively similar to the one shown in Fig. 1(a), with Fermi energy  $E'_F$ , indicating an insulating ground state.<sup>17</sup> The addition of the diagonal hopping terms distorts the bands allowing the stabilization of metallic stripes.<sup>5</sup>

Although the mean-field results mentioned above are very instructive, it is not clear that they represent the true ground state of the system. In addition, numerical studies are very difficult to perform directly in the Hubbard model. However, we have shown that the easier-to-study spin-fermion model captures many of its properties.<sup>8</sup> We have also observed that the addition of negative diagonal hopping parameters to the spin-fermion model with absolute values larger than  $0.05t$  destabilize the striped ground state on a square lattice.<sup>18</sup> This is the reason why, in spite of the encouraging mean-field results of Ref. 5, we will not show data here for finite diagonal hoppings.

In order to compare the schematic results of Fig. 1(a) with those of the spin-fermion model it has to be considered that antiferromagnetic models tend to have symmetrical band structures below and above the antiferromagnetic gap. Just as the conduction and valence bands described above are caused by an AF splitting, we should expect that the midgap

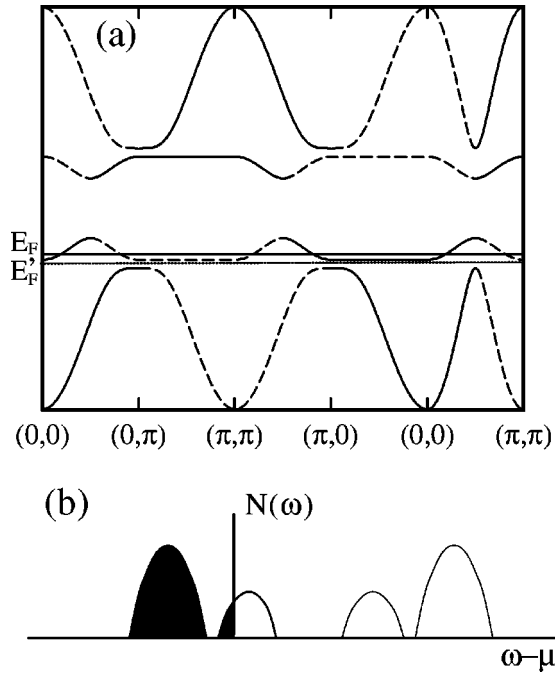


FIG. 2. (a) Schematic band structure along the path  $(0,0) - (0,\pi) - (\pi,\pi) - (\pi,0) - (0,0) - (\pi,\pi)$  in the FBZ for an AF system with a split midgap band associated to metallic quarter-filled vertical stripes with  $\langle n \rangle = 0.875$ .  $E_F$  indicates the position of the Fermi energy and shadow bands are indicated by a dashed line.  $E'_F$  indicates the position of the Fermi energy in the case of empty stripes. (b) The corresponding density of states.

band will itself be split in the same way. In our schematic model the energy of the split midgap band is given by  $E_m^\pm = \pm \sqrt{(t' \cos k_y)^2 + \Delta'^2}$ , where  $2\Delta'$  is the gap between the two bands. The expected band structure, using  $\Delta' = 0.5$  and  $t' = 0.7$ , is schematically shown in Fig. 2(a). This indicates that for vertical stripes, midgap spectral weight will appear close to the valence band around  $(\pi, 0)$ , while only shadow, and thus much weaker, spectral weight will appear around  $(0, \pi)$ . The observed midgap band should not disperse from  $(0, 0)$  to  $(\pi, 0)$ , but it will disperse from  $(\pi, 0)$  to  $(\pi, \pi)$ . It is also clear that very little midgap spectral weight will be observed along the diagonal direction for  $k$  larger than  $\pi/2$  since the shadow bands are not intense. In this naive picture, the Fermi surface will be similar to the one shown in Fig. 1(b) if  $E_F$ , in Fig. 2(a), is the Fermi energy.<sup>19</sup> As before, no FS will be observed if the Fermi energy is  $E'_F$  in Fig. 2(a). The DOS, on the other hand, will look qualitatively different from the one displayed in Fig. 1(c). Two midgap bands will appear, instead of one, as shown in Fig. 2(b).

A problem with the naive schematic picture that we just discussed is that, as can be observed in Fig. 2(b), the DOS does not have a pseudogap at the chemical potential, which is a feature experimentally observed in the cuprates. In our schematic scenario, a pseudogap would be observed if the midgap states and the valence band overlap each other. The resulting band structure is shown in Fig. 3(a). In this case, though, the Fermi surface would have an electronlike contribution coming from the valence band [dotted line in Fig.

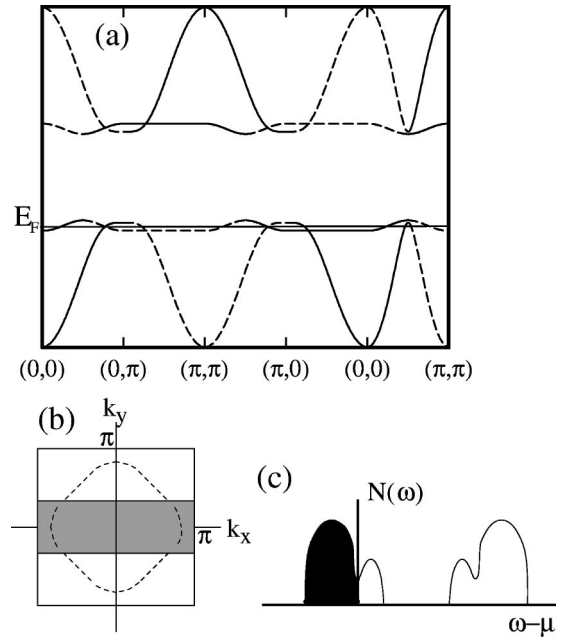


FIG. 3. (a) Schematic band structure along the path  $(0,0) - (0,\pi) - (\pi,\pi) - (\pi,0) - (0,0) - (\pi,\pi)$  in the FBZ for an AF system with overlapping midgap and valence (conduction) bands associated to metallic vertical stripes with overall  $\langle n \rangle = 0.875$ .  $E_F$  indicates the position of the Fermi energy and shadow bands are indicated by a dashed line. (b) Fermi surface corresponding to the band structure shown in (a). (c) The corresponding density of states.

3(b)], superimposed to a FS qualitatively similar to the one shown in Fig. 1(b) due to the partial filling of the midgap band, denoted by the full lines in Fig. 3(b). The resulting DOS, with a pseudogap at the chemical potential, is shown in Fig. 3(c). We would like to point out that although here we have presented the simplest case of band overlapping, it is also possible that the two bands would merge in which case a single FS would be observed.

## IV. RESULTS

### A. Half filling

Let us consider now the similarities and differences between the schematic results described in the previous section and those arising from the spin-fermion model. In Figs. 4(a) and 4(b) the spectral function along the main directions in the FBZ is shown for the undoped  $\langle n \rangle = 1$  spin-fermion model on an  $8 \times 8$  cluster. The dispersion of the main peaks in  $A(k, \omega)$  gives rise to the band structure presented in Fig. 4(c), in which a valence and conduction band separated by the AF gap appear. The shadow bands associated with the AF order are indicated by the dashed line in Fig. 4(c). The ground state is invariant under rotations in  $\pi/2$ , i.e., the features along the direction  $(0,0) - (0,\pi)$  are identical to those along  $(0,0) - (\pi,0)$ . The DOS showing the valence and conduction bands separated by the AF gap is displayed in Fig. 4(d). The chemical potential is in the middle of the gap indicating that the system is an insulator. The results shown here are to be expected for an AF insulator, and they dem-

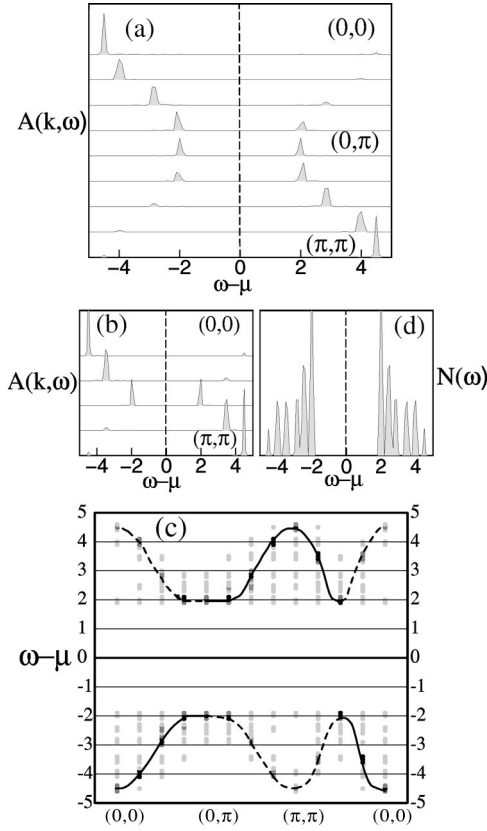


FIG. 4. Spectral function for the undoped spin-fermion model on an  $8 \times 8$  lattice as a function of  $\omega - \mu$ . (a) Along the path  $(0,0) - (0,\pi) - (\pi,\pi)$ ; (b) along the path  $(0,0) - (\pi,\pi)$ ; (c) the band structure obtained from (a) and (b). The lines indicating the main bands are to guide the eye. Dashed lines indicate shadow bands. Darker points indicate higher spectral weight; (d) the density of states  $N(\omega)$  vs  $\omega - \mu$ .

onstrate that the spin-fermion model with classical localized spins properly reproduces the main physics of such a state.

### B. $\langle n \rangle = 0.935$

In the MC simulations of the spin-fermion model, holes added to the system tend to align forming horizontal or vertical stripes, as discussed in previous literature.<sup>8</sup> Studying  $8 \times 8$  and  $12 \times 12$  systems it was observed that for  $x$  less than  $1/L$  holes doped ( $L$  is the side of the square cluster) the system remains an insulator. As an example, in Fig. 5 we present  $A(k, \omega)$  along the main directions in the FBZ for  $\langle n \rangle = 0.937$ , i.e., when four holes are introduced on the  $8 \times 8$  system.

In Figs. 5(a) and 5(b) it can be seen that spectral weight is transferred from the valence and conduction bands to the middle of the gap, creating two midgap bands shaded in black in Figs. 5(a) and 5(b), similarly to the second schematic model described in Sec. III. In the results shown here, the four doped holes are aligned vertically and, as expected, the spectral weight associated with the holes comes from the valence band, and it is located around  $(\pi, 0)$  in momentum space [Fig. 5(b)]. A redistribution of spectral weight, shaded in black in Fig. 5(a), is also observed close to the conduction

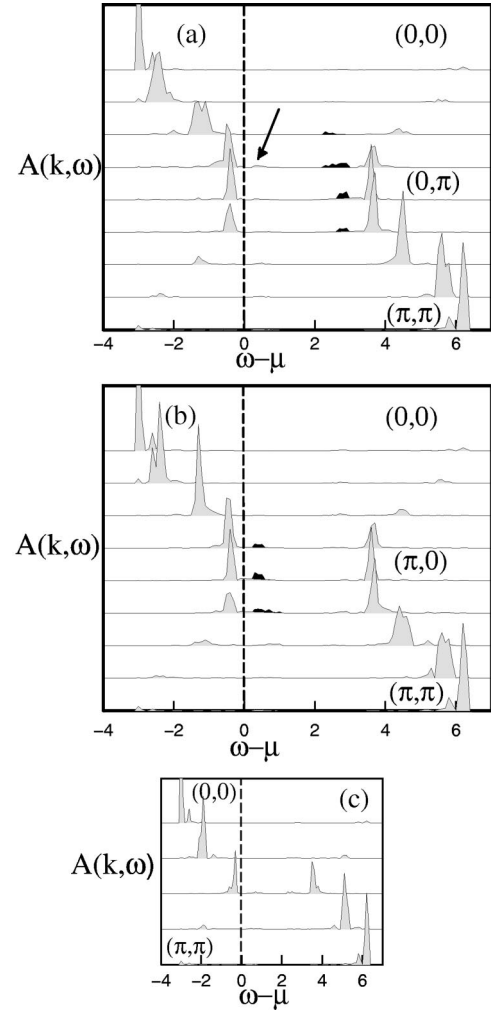


FIG. 5. Spectral function for the spin-fermion model with  $\langle n \rangle = 0.937$  on an  $8 \times 8$  lattice, with holes aligned along the vertical axis forming a straight segment. The midgap states are shaded in black. (a) Along the path  $(0,0) - (0,\pi) - (\pi,\pi)$ . The arrow indicates the midgap shadow states with nearly negligible weight; (b) along the path  $(0,0) - (\pi,0) - (\pi,\pi)$ ; (c) along the path  $(0,0) - (\pi,\pi)$ .

band around  $(0,\pi)$ . Only a negligible shadow weight, indicated with an arrow in Fig. 5(a), appears close to the valence band around  $(0,\pi)$ . It has been checked that, as expected, when the holes are aligned horizontally the states close to the valence (conduction) band are located close to  $(0,\pi)$  [ $(\pi,0)$ ]. Also in agreement with the schematic picture, we observe that the lower midgap states disperse along  $(\pi,0) - (\pi,\pi)$ , but not along  $(0,0) - (0,\pi)$ . A somewhat unexpected result though is that the low midgap spectral weight around  $(0,0)$  is negligible, and the same occurs along the diagonal direction. Thus, only states with momenta close to  $(\pi,0)$  and  $(0,\pi)$  contribute appreciably to the midgap bands in the spin-fermion model, in contrast with the schematic model of the previous subsection in which all the momenta participated.

The resulting band structure is shown in Fig. 6(a) and the DOS is presented in Fig. 6(b). This band structure is remi-



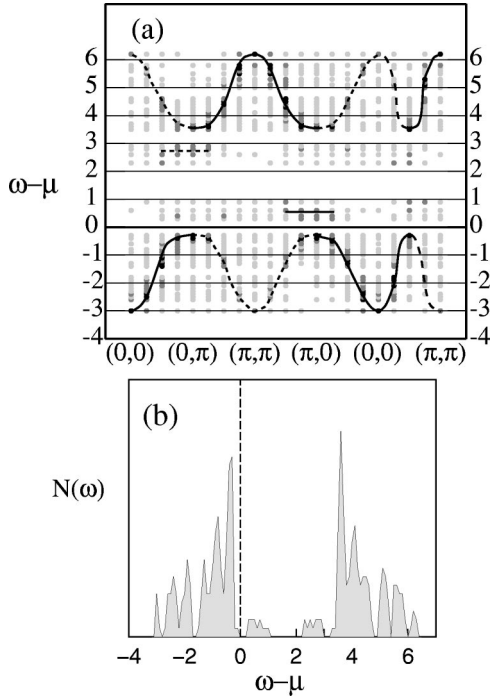


FIG. 6. Band structure for the spin-fermion model with  $\langle n \rangle = 0.937$  on an  $8 \times 8$  lattice obtained from the data in Fig. 5. (a) Along the path  $(0,0) - (0,\pi) - (\pi,\pi) - (\pi,0) - (0,0) - (\pi,\pi)$  in the FBZ. The valence, conduction, and midgap bands are indicated with lines to guide the eye. The dashed lines connect points with very small spectral weights that define shadow bands. (b) The density of states  $N(\omega)$  vs  $\omega - \mu$ .

niscent of the one described in Fig. 2 for vertical insulating 1D stripes in an antiferromagnetic background. The chemical potential is in a gap between the lower midgap band, associated to the doped holes in the stripes, and the valence band. The state is an insulator since the midgap bands are above the chemical potential. ARPES results for LSCO (Ref. 3) also detect an insulating ground state at low doping.

The symmetry under  $\pi/2$  rotations is clearly broken due to the vertical stripe of holes. However, independent MC simulations, using different random initial spin configurations, provide outputs with vertical or horizontal stripes indicating that the two states are degenerate. As more holes are added to the system in the insulating regime, spectral weight is transferred from the valence and conduction bands to the midgap states.

### C. $\langle n \rangle = 0.875$

At  $\langle n \rangle = 0.875$ , which corresponds to eight holes on the  $8 \times 8$  lattice, one stripe is stabilized in the ground state. A very important issue is whether the system is an insulator, as in the early mean-field results,<sup>17</sup> or metallic as suggested by the experimental data.

The electronic density of the stripes observed in the spin-fermion model is  $\sim 0.5$ ,<sup>8</sup> in agreement with the experiments, but there is a slight reduction in the density of all the sites of the lattice indicating that, on average, four holes are located at the stripe, while the other four are spread in the system.

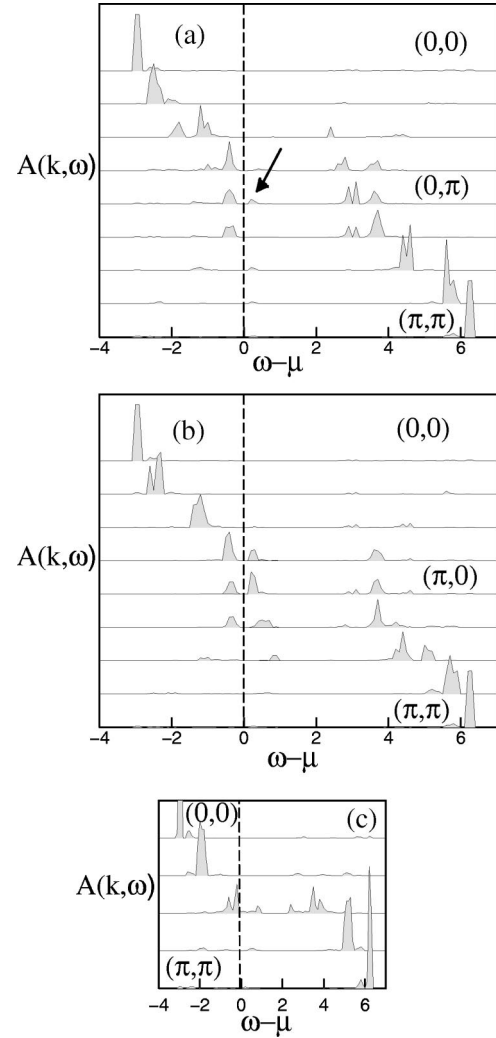


FIG. 7. Spectral function for the spin-fermion model with  $\langle n \rangle = 0.875$  on an  $8 \times 8$  lattice. (a) Along the path  $(0,0) - (0,\pi) - (\pi,\pi)$ . The arrow indicates the midgap shadow weight; (b) along the path  $(0,0) - (\pi,0) - (\pi,\pi)$ ; (c) along the path  $(0,0) - (\pi,\pi)$ .

We will discuss this point in more detail below. Notice that this is different from the picture emerging from experiments performed in Nd-doped LSCO (Ref. 2) in which two stripes rather than one would be expected to be observed in the situation that we are discussing, since the holes are assumed to be located exclusively in the quarter-filled stripes and not in the background. This could be a drawback of this model since the incommensurability pattern for LSCO is similar to the Nd-doped material mentioned above.<sup>20</sup> However, it is not clear that all the cuprates follow the same pattern.<sup>21</sup> The spectral functions in the FBZ are shown in Fig. 7 and they correspond to the case in which the stripe is vertical. The same results, exchanging  $k_x$  with  $k_y$ , were obtained for the case of a horizontal stripe. In Fig. 7(a) it can be observed that the lower midgap states only have very small shadow weight, indicated with an arrow, around  $(0,\pi)$ , as expected from the schematic model, and the valence band remains below the chemical potential. Thus, it appears that there is no FS along this direction.

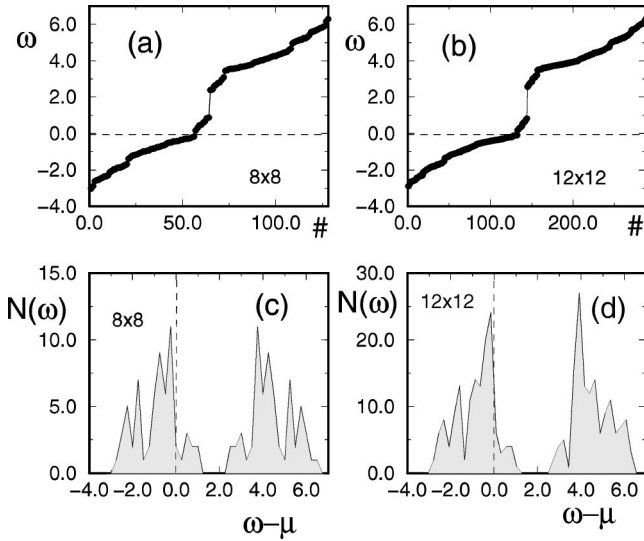


FIG. 8. (a) Eigenvalue distribution for a snapshot configuration on an  $8 \times 8$  cluster with a vertical stripe; (b) same as (a) but for a  $12 \times 12$  cluster; (c) density of states obtained from (a); (d) density of states obtained from (b).

Along the  $(0,0) - (\pi,0) - (\pi,\pi)$  direction depicted in Fig. 7(b), on the other hand, the valence band and the lower mid-gap band are very close to each other. On the  $8 \times 8$  system [Fig. 7(b)], there seems to exist a very small gap in between the valence and the midgap band that would indicate insulating behavior. However, we need to establish whether this gap is real or an artifact of the small lattice that we are studying. To explore this issue we studied the eigenvalue distribution of the Hamiltonian defined in Eq. (1) for several configurations of the spin variables (snapshots) whose ground state had one stripe on  $8 \times 8$  [Fig. 8(a)] and  $12 \times 12$  [Fig. 8(b)] systems. We observed that the eigenvalue distribution changes very little for the different snapshots. On the  $8 \times 8$  system a very small gap in the eigenvalue distribution was observed at the chemical potential indicated with a dashed line in Fig. 8(a). As expected, there are eight eigenstates forming the lower midgap states associated with the number of holes in the system.

For the  $12 \times 12$  system [Fig. 8(b)] the gap between the lower band and midgap states is smaller. The number of eigenstates per energy interval provides the density of states for the snapshot. A histogram of the eigenvalue distribution provides an estimation of the DOS. These histograms, using an energy interval equal to  $0.04t$ , are shown in Fig. 8(c) for the  $8 \times 8$  system and in Fig. 8(d) for the  $12 \times 12$  cluster. In both cases the chemical potential is very close to a pseudogap in the DOS located between the valence and lower midgap bands, as experimentally observed in the cuprates.<sup>22</sup>

Thus, combining the results in Figs. 7 and 8 we infer that, in this case, both the valence and the low midgap bands merge and will contribute to the Fermi surface. It is not possible to detect the position of the FS precisely due to the flatness of the overlapped bands close to  $(\pi,0)$ . Our data are consistent with either a FS at  $(\pi - \delta, 0)$  or at  $(\pi, \delta)$ , where  $0 \leq \delta < 3\pi/4$ . Notice that the dispersive behavior of the mid-

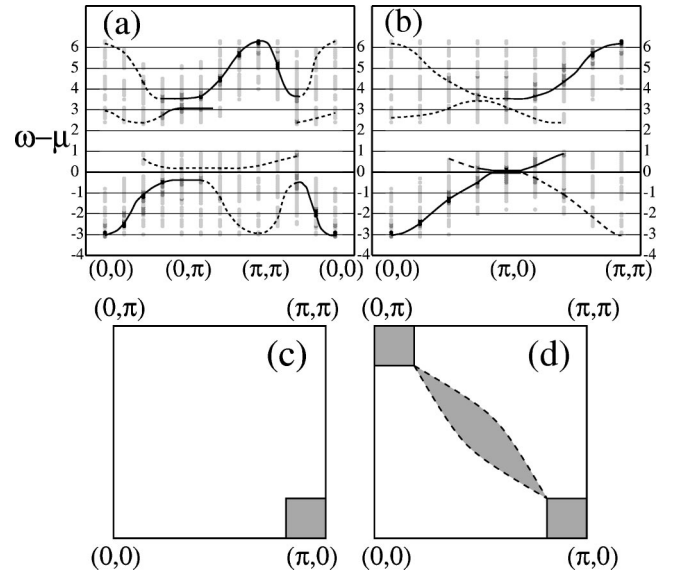


FIG. 9. Band structure for the spin-fermion model with  $\langle n \rangle = 0.875$  on an  $8 \times 8$  lattice obtained from the data in Fig. 5. (a) Along the path  $(0,0) - (0,\pi) - (\pi,\pi) - (0,0)$  in the FBZ; (b) along the path  $(0,0) - (\pi,0) - (\pi,\pi)$ ; (c) possible FS obtained from the data in Fig. 7; (d) possible FS obtained by combining the data for vertical and horizontal stripes. The solid lines indicate an actual FS, while the dashed line indicates a gapped region or very weak FS.

gap states is the type expected for vertical stripes in the schematic system, although the dispersion is small.

A similar analysis looking at Fig. 7(c) shows that a FS along the diagonal of the FBZ, i.e., from  $(0,0)$  to  $(\pi,\pi)$ , does not exist. The valence-band quasiparticle peak that is well defined at  $(0,0)$  becomes incoherent just below the chemical potential for momentum  $(\pi/2, \pi/2)$ , and it is almost touching the Fermi energy. The midgap states, as expected, have only shadow spectral weight.

The band structure arising from Fig. 7 is presented in Figs. 9(a) and 9(b) and the possible FS due to the vertical stripe is shown in Fig. 9(c). The shadowed region indicates its possible location and the solid lines running from  $(7\pi/8, 0)$  to  $(7\pi/8, \pi/8)$  and  $(\pi, \pi/8)$  to  $(7\pi/8, \pi/8)$  denote its two approximate extreme positions.

In Fig. 9(d) we show the possible FS obtained as a superposition of the results for horizontal and vertical stripes. It is an incomplete FS that could close either around  $(0,0)$  or  $(\pi,\pi)$  [solid line in Fig. 9(d)]. We could not determine if the surface is closed or open but away from  $(\pi,0)$  and  $(0,\pi)$  the spectral weight is weak and incoherent. The possible extreme positions of this weaker FS (or gap) is indicated with dashed lines in Fig. 9(d). The FS closing around  $(\pi,\pi)$  has been observed in underdoped LSCO (Ref. 3) and Bi2212.<sup>15,23</sup> The observation of a FS closing around  $(0,0)$  is controversial. According to Ref. 15 it appears in Bi2212 at 32.3 eV photon energy, while Ref. 23 interprets similar data as indicating no changes in the shape of the FS.

Our results are also in agreement with the LSCO data showing a weak or no FS along the diagonal in the underdoped regime.<sup>3</sup> ARPES data seem to indicate a FS along the diagonal direction in Bi2212,<sup>15</sup> but we believe that inverse

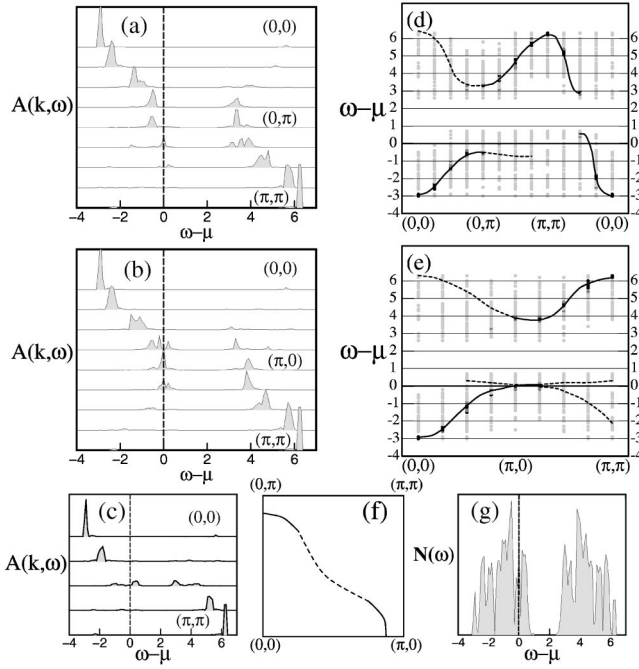


FIG. 10. Spectral functions for the spin-fermion model with  $\langle n \rangle = 0.81$  on an  $8 \times 8$  lattice. (a) Along the path  $(0,0) - (0,\pi) - (\pi,\pi)$  in the FBZ; (b) along the path  $(0,0) - (\pi,0) - (\pi,\pi)$ ; (c) along the path  $(0,0) - (\pi,\pi)$ ; (d) band structure along the path  $(0,0) - (0,\pi) - (\pi,\pi) - (0,0)$ ; (e) along the path  $(0,0) - (\pi,0) - (\pi,\pi)$ ; (f) FS obtained by combining the data for vertical and horizontal stripes. The dashed line indicates a very weak FS; (g) the density of states.

ARPES data would be necessary to rule out the existence of a gap. In our results the existence of the gap becomes clear after observing the behavior of the spectral weight in the valence band and the midgap band above  $\mu$ .

#### D. $\langle n \rangle = 0.80$

Next we will study how the band structure evolves as the system is doped further away from half filling. At  $\sim 20\%$  doping it is possible to determine that the FS closes around  $(0,0)$ . The symmetry under rotations is still spontaneously broken, but the potential barrier separating vertical and horizontal stripes appears to be lower than for lighter doping. As a result, some features due to horizontal configurations appear in the spectral functions presented here, which corresponds to a ground state with mostly vertical charge inhomogeneities.

The spectral functions along the main directions in the FBZ are shown in Figs. 10(a)–10(c), and the corresponding band structure is in Figs. 10(d) and 10(e). As in the previous case, a gap rather than a FS is observed close to  $(0,\pi)$  [Figs. 10(a) and 10(d)].<sup>24</sup> Close to  $(\pi,0)$  the valence and midgap bands overlap each other where the FS seems to be located [Figs. 10(b) and 10(e)]. The FS along the diagonal is still inexistent or very weak since the spectral weight at  $(\pi/2, \pi/2)$  is incoherent [Fig. 10(c)].

The shape of the FS for the combined ground state (with vertical and horizontal incommensurability) is shown in Fig.

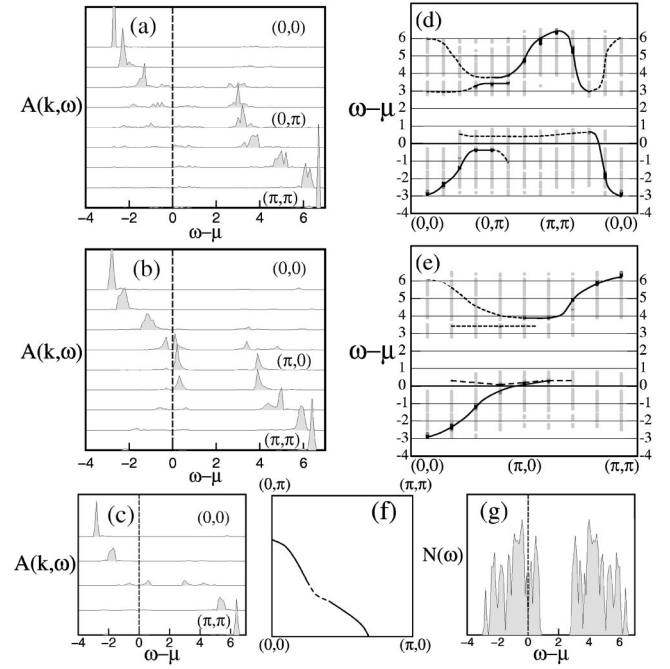


FIG. 11. Spectral functions for the spin-fermion model with  $\langle n \rangle = 0.75$  on an  $8 \times 8$  lattice. (a) Along the path  $(0,0) - (0,\pi) - (\pi,\pi)$  in the FBZ; (b) along the path  $(0,0) - (\pi,0) - (\pi,\pi)$ ; (c) along the path  $(0,0) - (\pi,\pi)$ ; (d) band structure along the path  $(0,0) - (0,\pi) - (\pi,\pi) - (0,0)$ ; (e) along the path  $(0,0) - (\pi,0) - (\pi,\pi)$ ; (f) FS obtained by combining the data for vertical and horizontal stripes. The dashed line indicates a very weak FS; (g) the density of states.

10(f). This FS was obtained by analyzing  $A(k, \omega)$  for all the available momenta in the FBZ. In Fig. 10(g) we present the DOS and it can be seen that the chemical potential is in a pseudogap.

#### E. $\langle n \rangle = 0.75$

When 16 holes are introduced in the system two parallel stripes are stabilized. The system is metallic and the FS closes around  $(0,0)$ . The spectral functions along  $(0,0) - (0,\pi) - (\pi,\pi)$  are shown in Fig. 11(a). It is clear that the valence band does not cross the chemical potential, and only shadow weight appears in the lower midgap band. Along  $(0,0) - (\pi,0) - (\pi,\pi)$ , presented in Fig. 11(b), the valence and low gap bands overlap and cross the chemical potential at  $k \sim (3\pi/4, 0)$ . The FS in the diagonal direction is weak because the spectral weight that crosses  $\omega = \mu$  is incoherent as can be seen in Fig. 11(c). The band structure corresponding to the case in which the stripes are vertical is shown in Figs. 11(d) and 11(e). The superposition of the two ground states (vertical and horizontal stripes) will give rise to a FS that closes around  $(0,0)$  as shown in Fig. 11(f). Clearly the chemical potential is located in a pseudogap in the density of states, as can be seen in Fig. 11(g).

#### F. $\langle n \rangle = 0.625$

With increasing doping the area of the FS is reduced. For  $\langle n \rangle = 0.625$  the symmetry under rotations is still broken. The

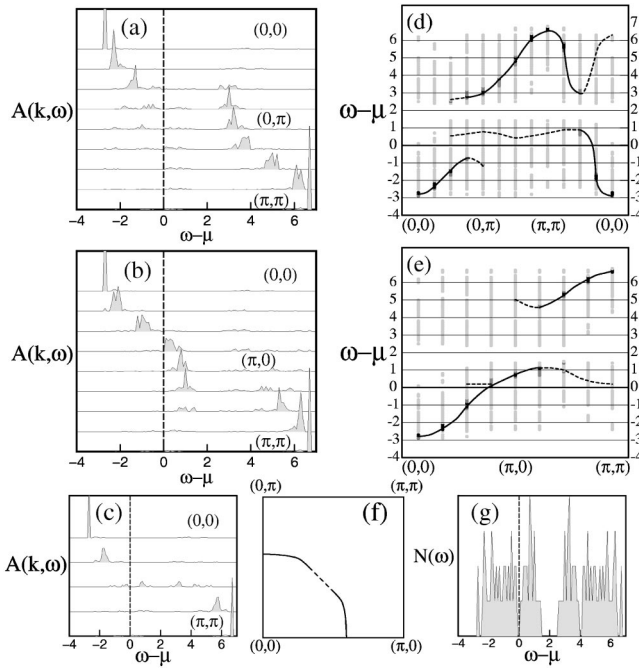


FIG. 12. Spectral functions for the spin-fermion model with  $\langle n \rangle = 0.625$  on an  $8 \times 8$  lattice. (a) Along the path  $(0,0) - (0,\pi) - (\pi,\pi)$  in the FBZ; (b) along the path  $(0,0) - (\pi,0) - (\pi,\pi)$ ; (c) along the path  $(0,0) - (\pi,\pi)$ ; (d) band structure along the path  $(0,0) - (0,\pi) - (\pi,\pi) - (0,0)$ ; (e) along the path  $(0,0) - (\pi,0) - (\pi,\pi)$ ; (f) FS obtained by combining the data for vertical and horizontal stripes. The dashed line indicates a very weak FS; (g) the density of states.

magnetic and charge incommensurability still form vertical or horizontal patterns. The spectral functions for the vertical pattern are shown in Figs. 12(a)–12(c). In Fig. 12(a) it can be seen that no FS is observed along  $(0,0) - (0,\pi) - (\pi,\pi)$ . Fig. 12(b) shows that the midgap and valence bands that had merged cross  $\mu$  below  $(3\pi/4, 0)$ . In the diagonal direction just below  $(\pi/2, \pi/2)$  incoherent weight crosses the chemical potential determining a weak FS [Fig. 12(c)]. The corresponding band structures are presented in Figs. 12(d) and 12(e) and the FS is shown in Fig. 12(f). The chemical potential is in a pseudogap as shown in Fig. 12(g).

### G. Analysis

The previous results indicate that as the electronic density varies from 1.0 to 0.625 a clear change in the band structure of the system occurs. Spectral weight for the momenta close to the chemical potential is transferred from the valence band to the lower midgap band. As a result, the chemical potential always appears in a pseudogap between the valence and the lower midgap bands. The bottom of the valence band, located at  $k = (0,0)$ , remains at an approximately constant distance from the chemical potential. This is very different from the mean-field studies<sup>5</sup> in which a rigid band structure is obtained and the chemical potential approaches the bottom of the valence band as holes are added. We believe that the main difference between our numerical results and mean

field is due to the fact that in the mean-field analysis the proposed striped background is always an almost perfect antiferromagnet, which physically is not accurate. Another important characteristic of the evolution of the band structure with doping is that while the gap between the valence and lower midgap bands closes becoming a pseudogap, the gap between the valence and conduction bands still exists even at 40% doping.

Another characteristic of the band structure in the metallic case is that for vertical incommensurability, the quasiparticle at  $(0,\pi)$  has lower energy than at  $(\pi,0)$  as can be seen in Figs. 9(a) and (b) and (d) and (e) of Figs. 10, 11, and 12. If we consider a two-dimensional system of free electrons with horizontal hopping  $t_x$  and vertical hopping  $t_y$ , the energy as a function of momentum is given by  $\epsilon_k = -2(t_x \cos(k_x) + t_y \cos(k_y))$ . It is clear that  $\epsilon(\pi,0) > \epsilon(0,\pi)$  if  $t_x > t_y$ . Although this comparison is naive, directly measured values of the electronic kinetic energy (KE) were found to be larger in the direction perpendicular to the stripes than along the stripes. The ratio between the parallel and perpendicular KE is of the order of 0.85 in the metallic phase. The difference in KE along and across the stripes may be justified by the fact that the stripes break the symmetry under rotations. This may indicate that, in the spin-fermion model, it is easier for the electrons to move in the direction perpendicular to the stripes rather than along them.

### V. THE PSEUDOGAP

The results presented in the previous section show that upon hole doping, a pseudogap between the valence and the lower midgap stripe-induced bands develops at the chemical potential in the density of states [see Figs. 8(c) and (d) and (g) of Figs. 10, 11, and 12]. This is a feature that has been observed experimentally both in the cuprates<sup>22</sup> and the manganites,<sup>25</sup> and it deserves to be understood in terms of the spin-fermion model.

The formation of a pseudogap at the chemical potential in the manganites has been explained in previous studies as arising from the coexistence of hole-poor antiferromagnetic insulating regions and hole-rich ferromagnetic clusters.<sup>26</sup> In Ref. 26 it was concluded that pseudogap behavior should be observed in any compound that is in a mixed-phase regime. Although the spin-fermion model does not present phase separation for the value of  $J$  studied in the present paper, it is clear that the “striped” ground state has mixed-phase characteristics, since the stripes are richer in holes than the background. A schematic picture of the hole distribution in the direction perpendicular to the stripes is shown in Fig. 13(a). The density of holes  $x$  in the direction perpendicular to the stripes is clearly nonuniform, and it is schematically shown in Fig. 13(b). We can represent this result using an “effective potential” for the holes that will be more negative at the stripes, as shown in Fig. 13(c). The states inside the wells generate the midgap bands along the direction parallel to the stripes in the Brillouin zone,  $(\pi,0) - (\pi,\pi)$  for vertical stripes. Clear quasiparticle peaks and maximum dispersion are expected along this direction since it is easier for the holes to move along the stripes. Along the direction perpen-



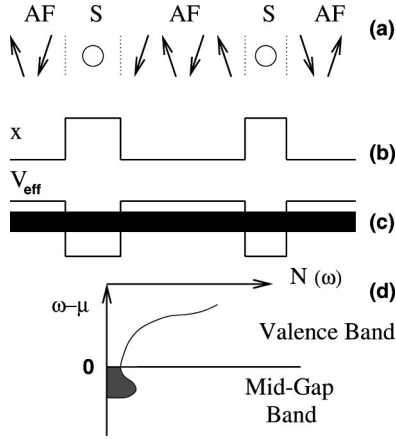


FIG. 13. Schematic explanation of the pseudogap formation upon hole doping in the spin-fermion model. In (a) a typical distribution of the AF background and stripes (S) reach in holes along the direction perpendicular to the stripes. In (b), the corresponding hole density  $x$  is sketched, showing that the holes are mostly located in the stripes. In (c), the effective potential felt by the holes is presented. The thick line indicates the midgap band populated with holes that develop. The resulting DOS with the chemical potential in the pseudogap is sketched in (d).

pendicular to the stripes, from  $(0,0)$  to  $(\pi,0)$  for vertical stripes, the holes move through tunneling between the potential wells or by fluctuations away from the stripe, effectively providing a width  $d$  to such stripes. This motion will generate a midgap band, schematically shown in Fig. 13(c). The electrons, on the other hand, will move mostly across the stripes, as discussed in the previous section and thus, a dispersive valence band would be expected. As a result of the formation of the midgap bands a pseudogap develops at the chemical potential in the DOS, as schematically shown in Fig. 13(d).

An important difference between the pseudogap in the spin-fermion model and the one observed in models for manganites is that in the latter the pseudogap is isotropic in momentum space. In the spin-fermion model, on the other hand, the pseudogap is clearly observed close to  $(\pi,0)$ , while a clear gap appears close to  $(0,\pi)$  (for vertical stripes) since the lower midgap band has only shadow weight here and the valence band has a lower energy than at  $(\pi,0)$ . This difference should be attributed to the one-dimensional nature of the stripes in the spin-fermion model. The incoherence of the spectral weight along the diagonal is, as mentioned above, due to the fact that diagonal hopping of electrons or holes is not particularly favored.

## VI. CONCLUSIONS

Summarizing, we have studied the spectral functions of the spin-fermion model, that has a ground state in which

added holes tend to form vertical and horizontal stripes, using unbiased numerical techniques. We have observed that doped holes contribute to the formation of midgap bands by modifying the valence and conduction bands associated to the insulator. The midgap bands arise from a dynamically generated effective potential that produces a nonuniform distribution of charge in the ground state. In the metallic regime the lower midgap and valence bands overlap each other, giving rise to a pseudogap in the density of states at the chemical potential, as observed in experiments for the cuprates. A pseudogap arising from inhomogeneities in the ground state has also been observed in previous investigations of models for manganites.

The ground state of the spin-fermion model appears to change from an insulator to a conductor with an incomplete FS when a single stripe gets stabilized, i.e., for a hole density  $x=1/L$ . In the conductor, electrons hop more easily in the direction perpendicular to the stripes. Thus, though the striped state in the spin-fermion model is not insulating, it appears that most of the electronic hopping occurs in the direction perpendicular to the stripes rather than along the stripes. At close to 20% doping, the FS clearly closes around  $(0,0)$ . These features are qualitatively similar to those observed in ARPES experiments. The band structure is not rigid, in disagreement with mean-field results, and it smoothly changes from insulating to conductor. Another interesting feature is the observation of well-defined quasiparticle peaks in  $A(k,\omega)$  that become incoherent as the chemical potential is approached indicating that the FS is very weak or it does not exist along the diagonal direction. This may indicate that the original quasiparticles in the  $(\pi/2,\pi/2)$  region are greatly affected by scattering from the stripes. Also close to  $(0,\pi)$  [ $(\pi,0)$ ] in the case of vertical (horizontal) stripes the chemical potential is in a gap. These features are related to the one dimensionality of the stripes. A similar behavior of the valence and midgap bands has been observed using a cluster perturbation theory for the  $t$ - $J$  model.<sup>27</sup>

Although part of our results disagrees with some of the theoretical models for stripes in the cuprates, we believe that this numerical study provides unbiased information on the dynamical properties of charge inhomogeneous ground states, which will be relevant to understand the behavior of materials whose inhomogeneous properties are just beginning to be unveiled experimentally.

## ACKNOWLEDGMENTS

We would like to thank G. Sawatzky and E. Dagotto for their useful comments. A.M. was supported by the NSF under Grant No. DMR-9814350. Additional support was provided by the National High Magnetic Field Lab and MARTECH.

- <sup>1</sup>S.-W. Cheong, G. Aeppli, T. Mason, H. Mook, S. Hayden, P. Canfield, Z. Fisk, K. Clausen, and J. Martinez, *Phys. Rev. Lett.* **67**, 1791 (1991); P. Dai, H. Mook, and F. Dogan, *ibid.* **80**, 1738 (1998); H.A. Mook, P. Dai, S. Hayden, G. Aeppli, T. Perring, and F. Dogan, *Nature (London)* **395**, 580 (1998).
- <sup>2</sup>J.M. Tranquada, J. Axe, N. Ichikawa, A. Moodenbaugh, Y. Nakamura, and S. Uchida, *Phys. Rev. Lett.* **78**, 338 (1997).
- <sup>3</sup>A. Ino, C. Kim, M. Nakamura, T. Yoshida, T. Mizokawa, Z.-X. Shen, A. Fujimori, T. Kakeshita, H. Eisaki, and S. Uchida, cond-mat/0005370 (unpublished).
- <sup>4</sup>E.S. Bozin, G. Kwei, H. Takagi, and S. Billinge, cond-mat/9907017 (unpublished).
- <sup>5</sup>M. Ichioka and K. Machida, *J. Phys. Soc. Jpn.* **68**, 4020 (1999).
- <sup>6</sup>T. Tohyama, S. Nagai, Y. Shibata, and S. Maekawa, *Phys. Rev. Lett.* **82**, 4910 (1999).
- <sup>7</sup>M. Salkola, V. Emery, and S. Kivelson, *Phys. Rev. Lett.* **77**, 155 (1996); M. Fleck, A. Lichtenstein, E. Pavarini, and A. Oles, *ibid.* **84**, 4962 (2000).
- <sup>8</sup>C. Buhler, S. Yunoki, and A. Moreo, *Phys. Rev. Lett.* **84**, 2690 (2000).
- <sup>9</sup>C. Buhler, S. Yunoki, and A. Moreo, *Phys. Rev. B* **62**, R3620 (2000).
- <sup>10</sup>P. Monthoux and D. Pines, *Phys. Rev. B* **47**, 6069 (1993); A. Chubukov, *ibid.* **52**, R3840 (1995); S. Klee and A. Muramatsu, *Nucl. Phys. B* **473**, 539 (1996).
- <sup>11</sup>J.R. Schrieffer, J. Low Temp. Phys. **99**, 397 (1995); B.L. Altshuler, L. Ioffe, and A. Millis, *Phys. Rev. B* **52**, 5563 (1995).
- <sup>12</sup>C.-X. Chen and H. Schüttler, *Phys. Rev. B* **43**, 3771 (1991).
- <sup>13</sup>S. Yunoki, J. Hu, A. Malvezzi, A. Moreo, N. Furukawa, and E. Dagotto, *Phys. Rev. Lett.* **80**, 845 (1998); E. Dagotto, S. Yunoki, A. Malvezzi, A. Moreo, J. Hu, S. Capponi, D. Poilblanc, and N. Furukawa, *Phys. Rev. B* **58**, 6414 (1998).
- <sup>14</sup>X.J. Zhou, P. Bogdanov, S. Kellar, T. Noda, H. Eisaki, S. Uchida, Z. Hussain, and Z.-X. Shen, *Science* **286**, 268 (1999).
- <sup>15</sup>D.L. Feng, W. Zheng, K. Shen, D. Lu, F. Ronning, J. Shimoyama, G. Gu, D. Van der Marel, and Z.-X. Shen (unpublished).
- <sup>16</sup>A. Kampf and J.R. Schrieffer, *Phys. Rev. B* **41**, 6399 (1990); **42**, 7967 (1990); S. Haas, A. Moreo, and E. Dagotto, *Phys. Rev. Lett.* **74**, 4281 (1995).
- <sup>17</sup>J. Zaanen and O. Gunnarsson, *Phys. Rev. B* **40**, 7391 (1989).
- <sup>18</sup>We are presently studying the model using ladders with positive as well as negative hopping.
- <sup>19</sup>The shadow band generates a very weak FS similar to the one in Fig. 1(b) rotated by  $\pi/2$ .
- <sup>20</sup>K. Yamada, C. Lee, K. Kurahashi, J. Wada, S. Wakimoto, S. Ueki, H. Kimura, Y. Endoh, S. Hosoya, G. Shirane, R. Birge-neau, M. Greven, M. Kastner, and Y. Kim, *Phys. Rev. B* **57**, 6165 (1998).
- <sup>21</sup>P. Dai, H. Mook, and R. Hunt, cond-mat/0011019 (unpublished).
- <sup>22</sup>T. Sato *et al.* (unpublished).
- <sup>23</sup>H.M. Fretwell, A. Kaminski, J. Mesot, J.C. Campuzano, M. Norman, M. Randeria, T. Sato, R. Gatt, T. Takahashi, and K. Kadawaki, *Phys. Rev. Lett.* **84**, 4449 (2000).
- <sup>24</sup>The small feature at the chemical potential for  $k=(\pi/4, \pi)$  in Fig. 10(a) comes from some configurations with horizontal charge inhomogeneities.
- <sup>25</sup>D. Dessau, T. Saitoh, C. Park, Z.-X. Shen, P. Vilella, N. Hamada, Y. Moritomo, and Y. Tokura, *Phys. Rev. Lett.* **81**, 192 (1998).
- <sup>26</sup>A. Moreo, S. Yunoki, and E. Dagotto, *Phys. Rev. Lett.* **83**, 2773 (1999).
- <sup>27</sup>M. Zacher, R. Eder, E. Arrigoni, and W. Hanke, *Phys. Rev. Lett.* **85**, 2585 (2000).